Supporting Information:

Active Trans-Plasma Membrane Water Cycling in Yeast is Revealed by NMR

Yajie Zhang, Marie Poirier-Quinot, Charles S. Springer, Jr., and James A. Balschi

Methods and Materials

Yeast suspensions with increasing [RR_e]: Yeast suspensions at 30% wet wt/vol in minimal medium were bubbled with 95% O_2/5% CO_2 (n =2) or 95% N_2/5% CO_2 (n=1) for 1.5 hours before the first ^1H_2O T_1 IR measurement. In one suspension bubbled with 95% O_2/5% CO_2, 10 μmole of the uncoupler of oxidative phosphorylation, 2,4-dinitrophenol, (DNP) was added after 1.5 hour of O_2 bubbling, just prior to the first addition of RR_e. Serial addition of RR to the yeast suspensions resulted in the following [RR_e] (mM) values in the medium: 0, 0.3, 0.6, 0.9, 1.2, 1.8, 2.4, 2.9, 3.5, 4.7, 7.0, 9.3, 11.6, 16.1, and 20.5. The total volume increased by 18% by the end of the titration, which was accounted for in calculating [RR_e]. The IR data acquired at each [RR_e] were analyzed by 2SX fitting and relaxivity fitting as described below.

MR Measurements and Data Analyses: The 64 t_I delay increments between the 180° (composite) pulse and 90° RF pulses of the IR pulse sequence are as follows (s): 0.001, 0.002, 0.003, 0.004, 0.005, 0.006, 0.007, 0.008, 0.009, 0.01, 0.012, 0.014, 0.016, 0.02, 0.024, 0.028, 0.032, 0.036, 0.04, 0.044, 0.048, 0.052, 0.056, 0.064, 0.072, 0.08, 0.088, 0.096, 0.104, 0.112, 0.12, 0.128, 0.136, 0.144, 0.152, 0.16, 0.17, 0.18, 0.19, 0.2, 0.22, 0.24, 0.26, 0.28, 0.3, 0.32, 0.34, 0.36, 0.4, 0.44, 0.48, 0.52, 0.6, 0.68, 0.76, 0.84, 0.92, 1, 1.2, 1.4, 1.6, 2, 2.4, 2.8.

Relaxograms: A 1D Inverse Laplace Transform (ILT) written in Matlab (TwoDLaplaceInverse, Magritek Limited, Wellington New Zealand) of $[(M_Z(\infty) - M_Z(t_I))/2M_Z(\infty)]$ produced the longitudinal relaxogram, the apparent relaxation time constant (T_1') distribution. A two peak relaxogram yielded H_2O_i T_1' (T'_{1i}) and H_2O_e T_1' (T'_{1e}) values, where the T_1' was taken as the peak position. The apparent relative water mole fractions were taken as the relative peak area values. Peak positions and areas were determined using Matlab routines (MathWorks Inc, Natick, MA).

Extracting exchange parameters: As noted in the main manuscript, two different approaches for extracting exchange parameters from relaxographic data were employed. The first method, "2SX fitting," substitutes Eqs. (4 – 6) into the right hand side of Eq. (*7*)

$$[(M_Z(\infty) - M_Z(t_I))/2M_Z(\infty)] = a_L\exp(-t_IR_{1L}) + a_s\exp(-t_IR_{1s}) \quad \textbf{\textit{(7)}}$$ (main manuscript)

The values of τ_i, p_i, and r_{1e} with fixed values for R_{1i} and R_{1e0} are adjusted to match the IR time-course, $[(M_Z(\infty) - M_Z(t_I))/2M_Z(\infty)]$, observed at each [$RR_e$] value.

The second method, "relaxivity fitting," adjusts Eq. (*4*) and/or (*5)* to match the [RR_e]-dependence of the R_{1L} and/or R_{1S} obtained from the relaxograms (1, 2). Matlab was used for the 2SX and relaxivity fittings.

Results

Inversion Recovery (IR) Data. **Figure S1** displays plots of the t_I-dependence of $\log[(M_Z(\infty) - M_Z(t_I))/2M_Z(\infty)]$ from yeast suspensions with different $[RR_e]$ values: panel A for the aerobic (O_2) condition, and, panel B for the anaerobic (N_2) condition. These plots can be characterized with reference to Eq. (*7*). When $[RR_e]$ is sufficiently small (certainly below 0.5 mM), the decays exhibit good linearity; the recovery from inversion is monoexponential. When the equilibrium trans-plasma membrane water exchange NMR system is truly in the Fast-eXchange-Limit [FXL] condition, the relaxation is monoexponential and $R_1 = p_iR_{1i} + p_eR_{1e}$ (2). This is the situation for the 0 mM RR_e suspensions. If the system remained in the FXL condition, the value of R_1 would increase linearly with $[RR_e]$ (slope = r_{1e}). In the range of $[RR_e]$ values that the plots remain linear (but $[RR_e]$-dependence of $R_1 < r_{1e}$), the systems are in the Fast-eXchange-Regime [FXR] condition (2). When $[RR_e]$ is sufficiently large (> 1.2 mM, inverted triangles), the plots exhibit nonlinearity; the recovery from inversion is non-monoexponential and the system has clearly departed the FXR and entered the Slow-eXchange-Regime [SXR] condition (2). When $[RR_e]$ is 3.5 mM and greater, the recovery appears distinctly bi-exponential. At the largest $[RR_e]$ reached, 20.5 mM, the more slowly decaying component, with slope = $- R_1' = - R_{1L}$, represents mostly $^1H_2O_i$. A straight line extrapolated through this component's later points, will strike the ordinate at the value of a_L. The difference between this intercept and the top of the ordinate (unity) is, by definition, equal to a_S. The a_L and a_S are *apparent* population fractions. They are not equal to the intrinsic values, p_i and p_e, which must be extracted by 2X analysis. If sufficient $[RR_e]$ could be reached such that $a_L = p_i$, then the system would be in the Slow-eXchange-Limit [SXL] condition [4]. It is also clear from inspecting Fig. S1 that going in the other direction (removing RR_e) a_S is the component that vanishes as the system approaches the FXL. This is an important principle of 2SX analyses. Most importantly these plots show the crucial differences between the $[(M_Z(\infty) - M_Z(t_I))/2M_Z(\infty)]$ curves obtained from aerobic and anaerobic yeast suspensions. This is the active trans-membrane water cycling manifest in the raw data.

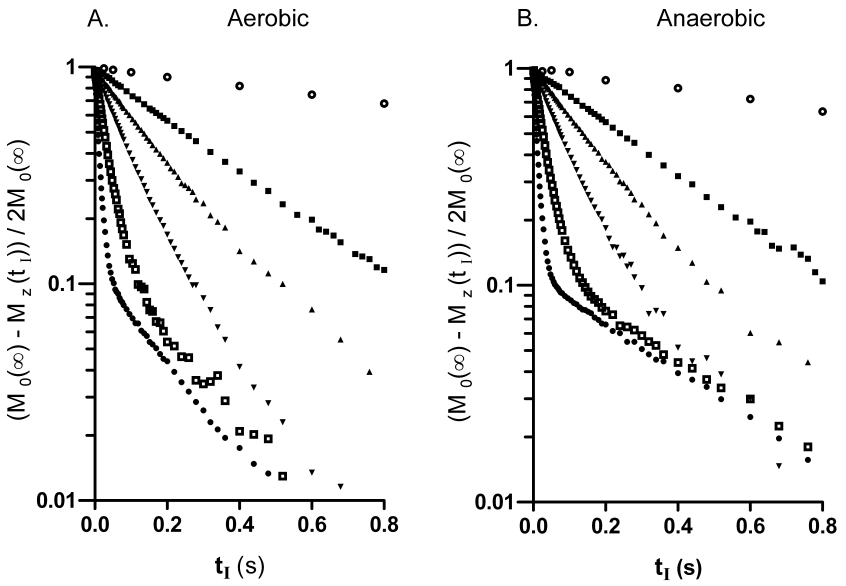

Figure S1 displays plots of the t_I-dependence of $\log[(M_0 - M_Z(t_I))/2M_0]$ of 30% w/v yeast suspensions with various $[RR_e]$ values (mM): 0 (○), 0.3 (■), 0.6 (▲), 1.2 (▼), 2.4(◆), 3.5(□), and 20.5 (●). **Panel A** displays results from the aerobic (O_2) condition. **Panel B** displays the results from the anaerobic (N_2) condition.

A stacked plot of T_1' relaxograms, which are the ILTs of the IR time-courses obtained from an aerobic yeast suspension (Fig. S1A) with increasing [RR_e] ([$GdDTPA_e^{2-}$]), is shown in **Figure** S2. As the [$GdDTPA_e^{2-}$] (oblique axis) increases from zero, the single ^1H_2O relaxographic peak shifts to smaller T_1' values. A second relaxographic peak emerges after [RR_e] reaches 2.9 mM. The peak, with the larger T_1' value, T_{1L}, hardly shifts with increasing [RR_e]. It represents mostly $^1H_2O_i$. The peak with the smaller T_1' value, T_{1S}, which continues to shift to smaller T_1' values, represents much of the $^1H_2O_e$ (2,3). The Fig. S2 relaxivity plot resembles that reported in Figure 4 of (1). Such results can be examined in the form of a relaxivity plot (R_{1S}' *vs.* [RR_e]), and be analyzed for water exchange with relaxivity fittings.

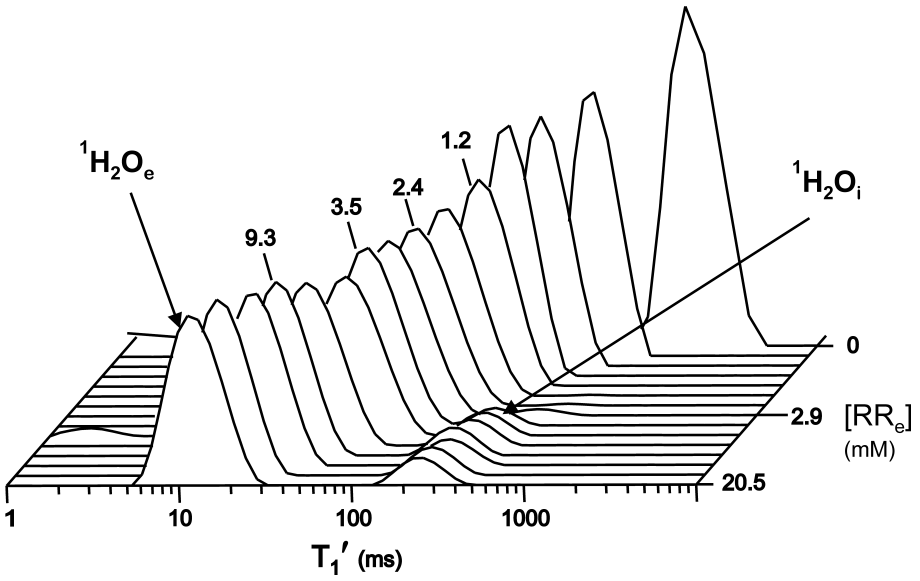

Figure S2. A stacked plot of ^1H_2O T_1 relaxograms, the Inverse Laplace Transforms (ILT) of the $(M_0–M_Z(t_I))/2M_0$ data, from a 30% w/v yeast suspension during aerobic (O_2) conditions. Aliquots of the RR, $GdDTPA^{2-}$, were sequentially added to the suspension. The extracellular RR concentration ([RR_e]) is plotted on the oblique axis. The horizontal axis plots the apparent T_1 (T_1') time constant (ms). The peak with the smaller T_1 value, T_{1S}, represents extracellular H_2O ($^1H_2O_e$); the peak with the larger T_1 value, T_{1L}, represents intracellular H_2O ($^1H_2O_i$).

Figure S3 displays a relaxivity plot, the [$GdDTPA_e^{2-}$]-dependences of the R_1' values extracted from the relaxograms (Fig. S2 and not shown). The plot for $GdDTPA^{2-}$ in cell-free (CF) minimal medium is also shown (triangles) for reference. The slope of its fitted (solid) line is the cell-free relaxivity (r_{1CF}), 4.43 (± 0.06) $s^{-1}mM^{-1}$. The ^1H_2O R_1 values for the small [RR_e] (< 2.9 mM) suspensions - before T_{1S}, T_{1L} peak separation (Fig. S2) - are plotted as open circles in Fig. S3. They fall on a (dashed) straight line that passes through the subsequent R_{1S} points, which are essentially the same for the aerobic (open squares) and anaerobic (filled squares) suspensions.

The T_{1L} peaks are distinct only when [RR_e] > 2.9 mM (Fig. S2). The R_{1L} values for yeast suspensions bubbled with O_2 (open diamonds in Fig. S3) and N_2 (filled diamonds) are different: R_{1L} (O_2) > R_{1L} (N_2) (Fig. S3B expands the origin of Fig. S3A). This is a further indication that the kinetics of equilibrium trans-plasma membrane water exchange are different under the aerobic and anaerobic conditions.

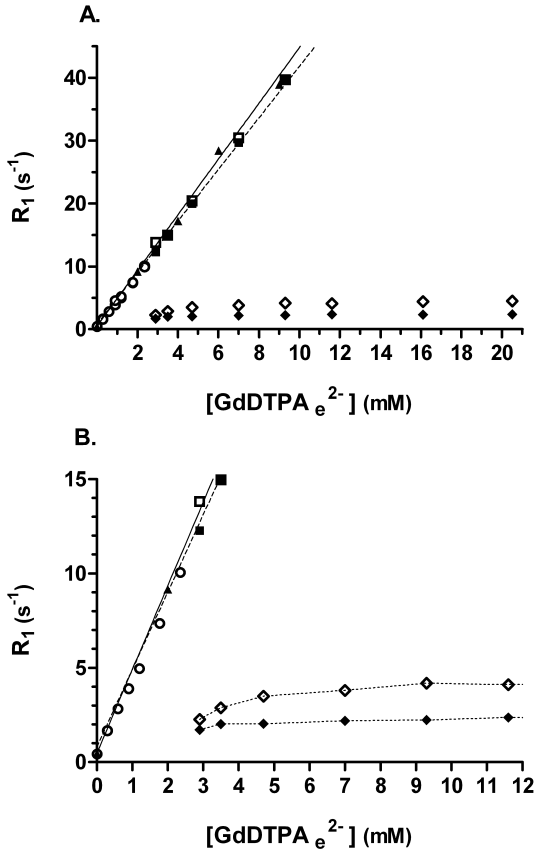

Figure S3, Panel A: displays a relaxivity plot, the longitudinal relaxation rate constant ($R_1 = T_1^{-1}$) *vs.* [$GdDTPA_e^{2-}$] for 30% w/v yeast suspensions. The suspension conditions were aerobic (O_2; (□) = R_{1S}; (◇) = R_{1L}) and, anaerobic (N_2; (■) = R_{1S}; (◆) = R_{1L}). The open circles represent the R_{1s} of the T_{1s} peaks before emergence of the T_{1L} peak; *i.e.*, when [RR_e] < 2.9 mM. The R_1 (▲) measured from cell free $GdDTPA^{2-}$ minimal medium solutions are also shown; the slope of the fitted line, the cell free relaxivity (r_{1CF}) equals 4.43 ± 0.06 s^{-1} mM^{-1}.

Panel B is an expansion of the panel A origin. The intracellular H_2O (H_2O_i) R_1 values of the yeast suspension during aerobic conditions (◇) are greater than those of the yeast suspension during anaerobic conditions (◆).

2SX Fitting and Relaxivity Analyses of IR data: An example of 2SX fitting method is shown in **Figure 1B**. This is the best fitted curve for the IR data set obtained from an anaerobic suspension of yeast with 9.3 mM $GdDTPA_e^{2-}$, the [RR_e] used for results in the main text. As is evident, the 2SX fitting approach involves fitting individual data sets, each a single [RR_e] IR measurement. In contrast, the relaxivity fitting method involves fitting either R_{1L}, Eq. (*4*) and/or R_{1S}, Eq. (*5*) to the appropriate R_1 measurements over a range of [RR_e] values. **Figure S4** displays the relaxivity fittings of the anaerobic yeast suspension RR_e titration relaxogram data (Fig. S2).

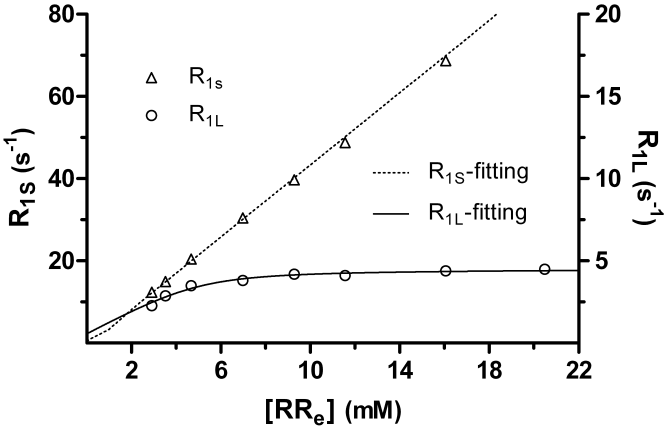

Figure S4. Relaxivity fitting of the yeast suspension relaxogram R_1 values, see Fig. S2. R_{1S} is plotted on left ordinate; R_{1L} is plotted on the right ordinate (note the scale difference). The parameter values, τ_i, p_i, and r_{1e}, returned from the independent R_{1S} and R_{1L} fittings are reported in **Table S3, O_2**.

To compare the two fitting methods, the RR_e titration results from three yeast suspensions were studied. A steady-state value for τ_i was assured by bubbling O_2 or N_2 for 1.5 hours before the first IR measurement. In one suspension, DNP was added after 1.5 hour of O_2 bubbling but prior to IR measurements. The first IR measurement was acquired before RR_e and then RR was serially added to the suspension with an IR measurement after each addition.

The IR data acquired for each measurement when $[RR_e]$ is sufficiently large (≥ 2.9 mM) that the recovery appears distinctly non-monoexponential were analyzed by 2SX fitting and the τ_i, p_i and r_{1e} values returned are listed in **Table S1**. The results from the IR data sets at 2.9, 3.5 and 4.7mM were different from those with $[RR_e] \geq 7$ mM and deemed unreliable: those at 4.7 mM do not deviate too badly. The results from 2SX fitting with $[RR_e] \geq 7$ mM were more consistent; and their mean τ_i, p_i and r_{1e} values are reported in **Table S2**. It may be that the data for $[RR_e] < 7$ mM (really, < 4.7 mM) are not sufficiently into the SXR condition: *i.e.*, the recoveries are not sufficiently non-monoexponential.

Table S1. 2SX fitting determined τ_i, p_i and r_{1e} values from IR time-course measurements of yeast suspensions with $[RR_e]$ increasing from serial addition.

	O_2			**O_2+DNP**			**N_2**		
$[RR_e]$ (mM)	τ_i (s)	p_i	r_{1e} (s^{-1} mM^{-1})	τ_i (s)	p_i	r_{1e} (s^{-1} mM^{-1})	τ_i (s)	p_i	r_{1e} (s^{-1} mM^{-1})
2.9	0.430	0.063	4.050	0.595	0.090	4.100	0.416	0.113	4.395
3.5	0.440	0.067	3.960	0.933	0.087	3.810	0.517	0.107	4.265
4.7	0.257	0.115	4.445	0.466	0.106	4.190	0.580	0.100	4.050
7.0	0.306	0.100	4.060	0.618	0.097	3.835	0.513	0.110	4.140
9.3	0.291	0.097	3.875	0.632	0.097	3.665	0.536	0.113	4.070
11.6	0.309	0.098	3.735	0.595	0.099	3.540	0.539	0.111	3.905
16.1	0.298	0.100	3.605	0.553	0.103	3.520	0.625	0.112	3.560
20.5	0.275	0.105	3.685	0.498	0.104	3.640	0.606	0.113	3.570

O_2 (aerobic conditions), O_2 + DNP (aerobic conditions with 2,4-dinitrophenol, an oxidative phosphorylation uncoupler), and N_2 (anaerobic conditions).

In the (main text) studies where there was only one $[RR_e]$ value, 9.3 mM, individual IR decays were analyzed by 2SX fitting, and the yeast were studied under aerobic conditions followed by anaerobic conditions (*i.e.*, Fig. 2). The mean τ_i value during the final 30 min of O_2 was 335 (± 36) ms, and, during the final 30 min of N_2 677 (± 57) ms. These values are also shown in **Table S2**, where comparison of these τ_i values to those of the $[RR_e]$ titration study finds them to be very similar for the O_2 conditions. Those from the titration N_2 (or O_2 +DNP) conditions displayed the same trend, *i.e.*, τ_i is larger under N_2 than O_2 conditions but not as much as observed in the constant $[RR_e]$ studies. This may result from the longer duration of the $[RR_e]$ titration study.

The p_i values returned by 2SX fitting were the equal for O_2 and O_2 +DNP conditions while the p_i under N_2 was 10% greater (**Table S2**). This suggests that the volume increase observed after the switch to anaerobic conditions (**Figure 2B**) is related to an increase in intracellular osmolytes caused by the lack of O_2 itself or, possibly, end products of anaerobic metabolism.

Relaxivity fittings of the R_{1L} and R_{1s} $[RR_e]$-dependencies from relaxograms with $[RR_e] \geq 2.9$ mM returned the τ_i, p_i, and r_{1e} values listed in **Table S3**. Comparing the values obtained from the R_{1L} and R_{1S} fittings for the three yeast suspensions shows the following: 1) the τ_i values are generally similar; 2) the p_i values are quite different with p_i (from R_{1L}) > p_i (from R_{1S}); and, 3) the r_{1e} values for each suspension are also quite different with r_{1e} (from R_{1L}) << r_{1e} (from R_{1S}) < r_{1CF}.

Table S2. **2SX fitting** determined average τ_i, p_i and r_{1e} values from IR time course measurements.

Yeast suspensions with $[RR_e] \geq 7$ mM	**O_2**	**O_2 + DNP**	**N_2**
τ_i (s)	0.30 (± 0.01)	0.58 (± 0.05)	0.56 (± 0.05)
p_i	0.100 (± 0.003)	0.100 (± 0.003)	0.111 (± 0.001)
r_{1e} (s^{-1} mM^{-1})	3.79 (± 0.18)	3.64 (± 0.13)	3.85 (± 0.27)
Yeast suspensions with $[RR_e] = 9.3$ mM			
τ_i (s)	0.33 (± 0.03)		0.68 (± 0.06)
p_i	0.073 (± 0.007)		0.093 (± 0.009)
r_{1e} (s^{-1} mM^{-1})	3.54 (± 0.13)		3.62 (± 0.08)
$R_{1i} = R_{1e0} = 0.48$ s^{-1}			

The mean (± SD) values from 2SX fitting with $[RR_e] \geq 7$ mM are from fitting results shown in Table S1A. The mean (± SD) values from 2SX fitting with $[RR_e] = 9.3$ mM are from Figure 2 (τ_i and p_i): O_2 from 65 – 125 min and N_2 from 125-265 min in manuscript.

Table S3. **Relaxivity fitting** determined τ_i, p_i and r_{1e} values from the $[RR_e]$-dependences of R_{1S} and R_{1L} when $[RR_e] \geq 2.9$ mM (the eight Table S1A suspensions).

	O_2		O_2 + DNP		N_2	
	R_{1L} fitting	R_{1S} fitting	R_{1L} fitting	R_{1S} fitting	R_{1L} fitting	R_{1S} fitting
τ_i (s)	0.311	0.309	0.445	0.515	0.502	0.5
p_i	0.125	0.05	0.191	0.052	0.29	0.123
r_{1e}(s^{-1} mM^{-1})	0.78	4.19	0.56	4.06	1	4.11
$R_{1i} = R_{1e0} = 0.48$ s^{-1}						

O_2 (aerobic conditions), O_2 + DNP (2,4-dinitrophenol, an uncoupler of oxidative phosphorylation), and N_2 (anaerobic conditions).

Comparing the results from the 2SX (**Table S2**) and relaxivity (**Table S3**) fittings of the RR titration data finds that both methods return similar τ_i values for the O_2 condition. The p_i values returned by 2SX fittings are generally consistent among the three different suspensions and smaller than the p_i values returned from the relaxivity fitting of the R_{1L} RR_e dependence. The 2SX fitting values are different from those of the R_{1S} relaxivity fitting. The r_{1e} values from the R_{1S} relaxivity fittings are closer to that of r_{1CF} (4.43 (± 0.06) s^{-1} mM^{-1}) than are the values obtained from 2SX fitting, which tend to be somewhat smaller.

Because the relaxivity fitting approach requires multiple $[RR_e]$ value suspension preparations (with different $[RR_e]$ values), the equilibrium trans-plasma membrane water exchange kinetics in the main text were quantified using the 2SX fitting approach. As noted above, the 2SX fitting

also returned more consistent values for τ_i, p_i, and r_{1e}. This is in agreement with our recent finding that, if IR data are of sufficient quality, it is more precise and accurate to fit a model to the data themselves than to their ILTs (4). Even so, relaxograms are invaluable for qualitative visualization (4). To increase accuracy in the studies reported in the main text, a single [RR_e] value of 9.3 mM was used. The water exchange system is clearly in the SXR with this [RR_e] value.

It is interesting to note that the mean r_{1e} value in **Table S2** is 3.76 $s^{-1}mM^{-1}$; 15% smaller than the r_{1CF} value. In an earlier RR titration study of yeasts, we found r_{1e} to be almost 40% smaller than r_{1CF} (1). Then and more explicitly later, we suggested that this might reflect exclusion of the RR^{2-} anion from the yeast periplasm, the space outside the plasma membrane but within the cell wall (2). Our result here is consistent with this hypothesis. Since the cell density employed in (1), 103% (w/v), was more than three times greater than that here, the periplasm would constitute a greater fraction of the aqueous space outside the yeast cell membrane than here. In (2) we noted that r_{1e} always enters the 2SX model in the $r_{1e}[RR_e]$ product, Eqs. *(4)-(6)*. Thus, $r_{1e}[RR_e]$ is analogous to a (thermodynamic) activity of RR_e, and r_{1e} to its activity coefficient (2). As such, r_{1e} can be very sensitive to the nature of the tissue molecular environment of the RR_e. It can increase when RR interacts with macromolecules that increase the RR molecular rotational correlation time constant (Proton Relaxation Enhancement), and it can decrease when RR is excluded from a tissue space, *e.g.*, for polyelectrostatic reasons, which is still freely accessible to water molecules that can also interact with RR molecules.

Ebselen treated yeast suspensions: In the studies shown in Figure 4A (manuscript), τ_i^{-1} increased after the O_2 switch in control yeast but not in ebselen-treated suspensions. The p_i value initially decreased after switching to O_2 in ebselen-treated and control cells (**Figure S5A**). At 16 min., the ebselen-treated cell p_i had returned to its anaerobic value, while the control cell continued to decrease.

The extracellular pH (pH_e) of control and ebselen-treated dense yeast suspensions (30% w/v) were measured before and after the transition from anaerobic (t = 0) to aerobic conditions (**Figure S5B**). The pH_e of control yeast suspension transiently decreases ~0.4 pH unit by 6 min after the oxygenation begins and then over the next 14 min it mostly recovers and increases ~0.4 pH unit (to pH_e = 6.09; t = 20 min). The pH_e of ebselen-treated dense yeast suspension also decreases ~0.3 pH unit, however, over the next 14 min pH_e continues to decrease another ~0.7 pH unit (to pH_e = 4.9; t = 20 min). The differences between control and ebselen-treated yeast suspensions are somewhat surprising. We had anticipated that the pH_e of ebselen-treated yeast suspensions would be relatively stable. Lower cell density ebselen-treated yeast suspensions (4% w/v) indeed do exhibit stable pH_e upon oxygenation (**Figure S5C**); while the pH_e of control yeast decreased and then increased. It is possible that the pH_e decrease is dominated by the efflux of organic anions (HCO_3^-) resulting from the aerobic metabolism. Since we find that ATP content and hence ATP production, is equal in ebselen-treated yeast they must also be generating CO_2 (and HCO_3^-). It is possible that in the ebselen-treated yeast this may be accompanied by H^+, or occurs as H_2CO_3, which would be membrane permeable. Extruded H_2CO_3 would lower the pH of extracellular medium. The $[H_e^+] > [H_i^+]$ gradient needed to establish the membrane potential is very small.

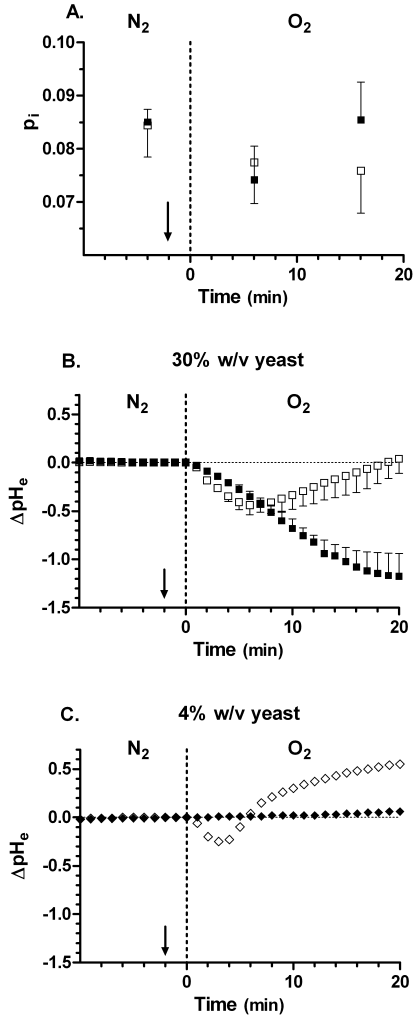

Figure S5.: The effect of changing the yeast plasma membrane H^+-ATPase activity before energizing the cells by switching from N_2 (anaerobic condition) to O_2 (aerobic condition) [at t = 0, dashed line]. At -2 min (vertical arrows) either DMSO solution of ebselen (2-phenyl-1,2-benzisoselenazol-3(2H)), an inhibitor of the plasma membrane H^+-ATPase or DMSO alone (control) was added to the suspension.

Panel A displays the p_i (□; n=4) for control and (■; n=5) for ebselen-treated 30% w/v yeast suspensions.

Panel B displays the ΔpH_e (ΔpH_e = [pH_e(t) - mean pH_e(t = -10 to 0)]) for 30% w/v control (□) (n=4) and ebselen-treated (■) (n=4) yeast suspensions. Mean (± SD).

Panel C displays the ΔpH_e for 4% w/v control (◇) (n=1) and ebselen-treated (◆) (n=1) suspensions.

References:

1. Labadie, C., J. H. Lee, G. Vetek, and C. S. Springer, Jr. 1994. Relaxographic imaging. J Magn Reson Ser B 105:99-112.
2. Landis, C. S., X. Li, F. W. Telang, P. E. Molina, I. Palyka, G. Vetek, and C. S. Springer, Jr. 1999. Equilibrium transcytolemmal water-exchange kinetics in skeletal muscle in vivo. Magn. Reson. Med. 42:467-478.
3. Li, X., W. Huang, E. A. Morris, L. A. Tudorica, V. E. Seshan, W. D. Rooney, I. Tagge, Y. Wang, J. Xu, and C. S. Springer, Jr. 2008. Dynamic NMR effects in breast cancer dynamic-contrast-enhanced MRI. Proc Natl Acad Sci USA 105:17937-17942.
4. Zhang, Y., M. Poirer-Quinot, C. S. Springer, Jr., and J. A. Balschi. 2010. Discrimination of intra- and extracellular $^{23}Na^+$ signals in yeast cell suspensions using longitudinal magnetic resonance relaxography. J Magn Reson 205:28-37.